

Computational Study of Thermal Changes during the Non-invasive Neuro-electrostimulation of the Nerve Structures in the Human Neck

Modelling Using Finite Element Method

Vladimir Kublanov¹, Mikhail Babich¹, Anton Dolganov¹, Fedor Kornilov² and Anna Sajler³

¹Research Medical and Biological Engineering Centre of High Technologies, Ural Federal University, Mira, 19, 620002, Yekaterinburg, Russian Federation

²N. N. Krasovskii Institute of Mathematics and Mechanics of the Ural Branch of the Russian Academy of Sciences, Sofia Kovalevskaya, 16, 620990, Yekaterinburg, Russian Federation

³Ural State Medical University, Department of Human Anatomy, Repina, 3, 620028, Yekaterinburg, Russian Federation

Keywords: FEM Modelling, Neuro-electrostimulation, Human Neck, SYMPATHOCOR-01 Device.

Abstract: In the article methodology of FEM stimulation of thermal effects, caused by neck-region neuro-electrostimulation was shown. Algorithm of the voxel model conversion to the 3-D objects represented as the complex of the STL-files was described. The evaluation of the temperature in the biological tissues is based on the association of the partial thermal changes, caused by the harmonics components of the pulsed neuro-electrostimulation signal. Features of the thermal changes in the neck region were considered for the neuro-electrostimulation by means of the current pulse field formed in the "SYMPATHOCOR-01" device. Results have shown that for modulation frequencies in range 45-55 Hz, duration of the partial pulses 25-30 us, current pulse amplitude less than 13 mA, the neuro-electrostimulation does not cause thermal changes higher than 0.1 K.

1 INTRODUCTION

Non-invasive portable neuro-electrostimulation devices are widely used in the contemporary medical practice. These devices use low-frequency pulse signals with single polarity for the stimulation. These devices are used to treat patients with exogenously-organic diseases of the central nervous system, anxiety and depressive disorders, atrophic diseases of the nervous system, and diseases accompanied by cognitive, sensory, motor and autonomic disorders. The peripheral nervous system is usually used as the target for devices exposure. Among the variety of the non-invasive devices, the multi-electrode systems are the most promising. The effectiveness of the multi-electrode systems arises from the spatial distribution of current pulses in the stimulation zone.

The "SYMPATHOCOR-01" is an example of such multi-electrode systems. Methods of the "SYMPATHOCOR-01" device clinical application implements the methodology of dynamic correction of the activity of the sympathetic nervous system (DCASNS) and provide correction of the autonomic

balance, determined by the ratio of activity of the sympathetic and parasympathetic divisions of the autonomic nervous system (ANS). The "SYMPATHOCOR-01" device is included in the State Registry of medical devices in Russia (registration certificates №FSR 2007/00757 from 28.09.2007), and instructions for its use were approved in August 1999, by head of the State control of the Quality, Efficiency, and Safety of Medicines and Medical Equipment Department of the Russian Ministry of Health (Kublanov, 2008a).

During the neuro-electrostimulation procedure via the "SYMPATHOCOR-01" device, Joule heating of electric currents cause local heating zones. Excessive heating of the biological tissues may change normal functioning in the local zones or cause thermal damage of tissue.

There is many papers that study heating processes of biological tissues during electrostimulation. However, as heating processes cannot be investigated *in vivo*, these processes are assessed by numerical solving of the Pennes equation (Bergman and Incropera, 2011) or by physical experiments (Su *et*

al., 2014). Yet implementation of physical experiments can be difficult.

Biological objects have a complex geometry. Therefore, numerical solving of the Pennes equation is usually performed by the finite element method (FEM) (Cao *et al.*, 2015). At present time, FEM modelling does not allow transient simulation of the pulsed current for frequency dependent characteristics of biological tissues. Therefore, it is advisable to produce decomposition of the pulse currents into Fourier series, to perform modelling of the harmonic components of the pulsed current, and to combine partial effects of the harmonic components.

The aim of the present work is to evaluate the tissue heating process formed during neuro-electrostimulation of the human neck by the field of the pulsed current.

2 MATERIALS AND METHODS

To evaluate the tissue heating process, voxel model of the human neck was used. In order to simplify the simulation procedure, it is appropriate to consider a pulse sequence as a superposition of harmonic components, determined by Fourier series.

In current work COMSOL Multiphysics (COMSOL Inc., USA) software was used for solution of the Pennes bioheat equation for heat transfer. Before the solution start, human body voxel model was transformed into the STL-files. Every STL-file represent particular 3-D biological object. For the voxel body model transformation, the in-house script was written in the Python language of with Anaconda distribution (Continuum analytics, USA).

After solution solving by means of the FEM, temperatures dependencies on the x, y, z spatial coordinates have been exported to *.csv files.

Further by means of the in-house script in the Python language with Anaconda distribution using the set of *.csv files, maximum thermal changes in the biological tissues of the human neck in dependence on amplitude, frequency and duration of the neuro-electrostimulation impulse signal were plotted.

2.1 “SYMPATHOCOR-01” Device Description

In the “SYMPATHOCOR-01” device for neuro-electrostimulation of the nerve structures, the spatially distributed rotating field of the current pulses is formed. The field is created between two

multi-electrode arrays, located on the left and right sides of the neck. The central electrode of each multi-electrode array serve as anode, and is placed on the projection of the cervical ganglia of the ANS. The other electrodes in the multi-electrode array are partial cathodes provide spatial patterns of the filed.

Partial current pulses, flowing from the anode of one electrode array to partial cathodes of another electrode array, form resulting current pulse filed. Each of the partial pulses have an amplitude and duration in the following ranges:

- the pulse amplitude varies from 0 to 15 mA;
- duration of each pulse ranges from 15 to 60 us.

Current pulse filed is modulated by frequency, that ranges from 5 to 150 Hz. In that case for a single period of the field formation, from 1 to 13 partial current pulses can be generated. Each pulse follows the previous one consequently.

The process of the thermal changes formation as the result of the neuro-electrostimulation is formed by set of partial current pulses, flowing between the anode and the partial cathodes. Therefore, for simulation formation of the current pulse field as the superposition of the processes, caused by the transition of the partial currents pulses between anodes and one partial cathode.

The partial current pulses used in the “SYMPATHOCOR-01” device has a very small duty-cycle varying from $75 \cdot 10^{-6}$ to $9 \cdot 10^{-3}$. Therefore 99% of the power is contained in first 2000 harmonics.

Low-frequency monopole pulse sequence of the signal, formed in the “SYMPATHOCOR-01” device, as any periodic signal can be decomposed into a Fourier series as a sum of harmonics.

$$f(t) = a_0 + \sum_{n=1}^{\infty} (a_n \cos(2\pi \frac{n}{T} t + \theta_n)), \quad (1)$$

where: t – time, $f(t)$ – neuro-electrostimulation signal in time domain, a_0 – amplitude of constant part of signal, n – number of harmonic component of the signal, a_n – amplitude of n -th harmonic component of the signal, T – period of signal repetition, θ_n – phase of n -th harmonic component of the signal.

On the other hand, according to the Parseval's theorem, the average power of the signal is the sum of the power spectral densities of the components, which does not depend on their phases (Arfken *et al.*, 2011).

$$P = \sum_{n=0}^{\infty} P_n, \quad (2)$$

where: P – average power of the signal, P_n – average power of n -th harmonic component of the signal.

According to the Newton's law of cooling, power is directly proportional to the thermal difference between body and its surroundings.

$$P = \frac{dQ}{dt} = h A \Delta T, \quad (3)$$

where: Q – thermal energy, h – heat transfer coefficient, A – heat transfer source area, ΔT – thermal difference between the body and its surroundings (Bergman *et al.*, 2011).

Thus, the total thermal difference between the body and its surroundings as a result of current pulses Joule heating can be determined as the sum of the partial thermal differences between the body and its surroundings caused by individual harmonic components.

$$\Delta T = \sum_{n=0}^{\infty} \Delta T_n, \quad (4)$$

where: ΔT_n – thermal difference between the body and its surroundings caused by n -th harmonic component of pulse signal.

Harmonic signals with constant amplitude were used for simulation. Thermal effect of each harmonic component was computed proportional to the ratio of the signal components and simulation components powers.

$$\Delta T_n = \frac{a_n^2}{b_n^2} \Delta T m_n, \quad (5)$$

where: b_n – harmonic signal amplitude used in FEM solution, $\Delta T m_n$ – thermal difference between the body and its surroundings obtained after FEM solution for n -th harmonic component of pulse signal.

Finally, the total thermal difference of biological tissues caused by the current pulses Joule heating is determined by the following equation.

$$\Delta T = \sum_{n=0}^{\infty} \frac{a_n^2}{b_n^2} \Delta T m_n. \quad (6)$$

2.2 Model Preparation

Model Duke from the Virtual Population ViP1 models has been used as the primary model of human body (Christ *et al.* 2010). The Duke model provides reliable information about the anatomy of the entire human body, obtained with the help of magnetic resonance imaging and the subsequent segmentation

of the results. This method of constructing the model provides high accuracy of the simulation results.

The Duke model is a 3-D matrix. Each element (voxel) of the 3-D matrix stores a value indicating whether an element belongs to a particular biological tissue. The model represents 77 types of various biological tissues. Geometric size of one voxel is 1 mm x 1 mm x 1 mm.

The whole body model has been truncated to the human's neck area, in accordance with papers goals. Truncated 3-D matrix has a size of 201 mm x 222 mm x 102 mm. Length and width of the truncated matrix fully include the cross-section of the human neck. Truncated matrix height is 7 times larger than the standard electrode used in the "SYMPATHOCOR-01" device for neuro-electrostimulation procedures. For these procedures, circular brass electrodes with 15 mm diameter and 0.2 mm thickness are used (Kublanov, 2008b). The boundaries of the model are far away enough from the electrode application site and have a minimal impact on the current distribution and the formation of local heating zones in the neck.

Cross-section of the 3-D human neck model matrix in the area of the electrodes placement is shown in Fig 1. At Fig. 1 pixels, representing the same biological tissue have the same brightness.

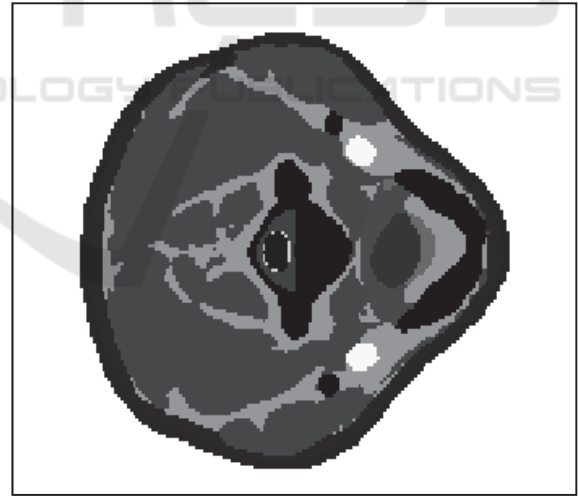


Figure 1: Cross-section of the three-dimensional human neck model.

The COMSOL simulation software has no possibility of using voxel models of geometric solids. Therefore, it is necessary to transform a voxel model to the format of 3-D models of objects, such as STL.

Block diagram of the algorithm for voxel models to STL format conversion is shown in Fig. 2. This

algorithm has been implemented in Python using the Anaconda distribution.

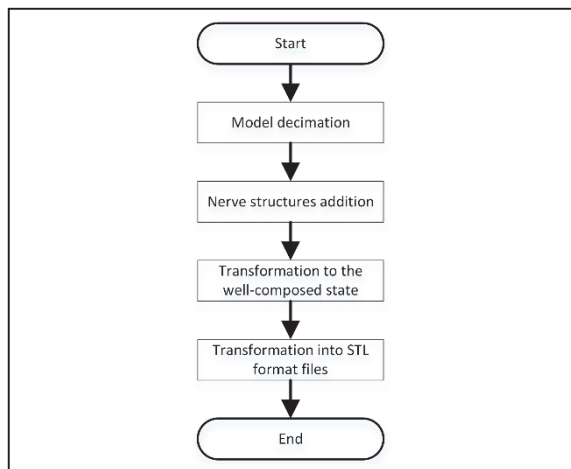


Figure 2: Block diagram of an algorithm for voxel models to STL format conversion.

For COMSOL simulation software it is necessary that objects do not contain zero thickness geometry. Therefore, the algorithm includes a step of bringing a voxel model to well-composed state. Feature of this step is the increase of the voxel 3D-matrix resolution. This leads to a significant increase of 3D-matrix elements and, as the result, significant increase of the requirements for computational resources. Pre-decimation of the original 3D matrix model was carried out for the optimization of computing resources.

In the first step of the conversion algorithm decimation (reduction in size) of 3-D voxel model of the neck by a factor of 3 is executed for each dimension. Decimation factor should be selected to be the smallest among all possible values, in a way that the number of elements obtained in the 3D-matrix does not cause difficulties in solution of the FEM model. Decimation procedure consists of the following steps:

- selection of the cube with the size $3 \times 3 \times 3$ voxels in initial 3D-matrix;
- picking of the most common value in the selected voxel;
- setting the most common value to appropriate place into decimated matrix.

As a result, the algorithm creates a decimated matrix comprising $(x/3) \times (y/3) \times (z/3)$ voxels in each dimension, where x, y, z the number of voxels in the initial 3D-matrix. The size of each voxel in the decimated 3D-matrix is increased to a value of 3 mm x 3 mm x 3 mm.

Cross-section of the human neck model after decimation is shown in Fig. 3. The vertical level of the image is selected the same as in Fig. 1. At Fig. 3 pixels, representing the same biological tissue have the same brightness.



Figure 3: Cross-section of the human neck model after decimation.

Second step of the conversion algorithm is the addition of the nervus vagus, sympathetic trunk, nervus hypoglossus, nervus accessories to the decimated neck model, in accordance with the anatomic atlas of Netter and Frank (Netter, 2010). In the original Duke model as well as in the model after decimation nerve formations in the neck are not represented. These nerve structures are the targets for the "SYMPATOKOR-01" neuro-electrostimulation, and therefore their presence in the model is needed.

At the third step of the conversion algorithm, decimated voxel 3D-matrix has been improved to a well-composed state. The criterion for well-composed state is the absence in the model geometry of zero thickness between geometric objects, consisting of a same biological tissue (Gonzalez-Diaz *et al.*, 2015).

Algorithm of the 3D-matrix improvement to the well-composed state consists of the following steps:

- interpolation of the 3D-matrix with the interpolation factor equaled to 3 for each dimension based on zero-hold method (Laughton and Warne, 2002);
- search for not well-composed pairs of voxels in the interpolated 3D-matrix;
- modification of voxels, neighboring with found not well-composed pairs so that the not well-composed pair will become well-composed.

Interpolation factor is set to 3 because this is the minimum value that will not cause a new not well-composed pairs by removing the old ones. The advantage of such algorithm is the preservation of the topology model from changes. Cross-section model of the well-composed human neck is shown in Fig. 4.



Figure 4: Cross-section model of the well-composed human neck.

The vertical level of the image is selected the same as in Fig. 1. At Fig. 4 points, consisting of the same biological tissue have the same brightness.

After decimation, interpolation, improvement to well-composed state steps the resulting 3D-matrix size was $201 \times 222 \times 102$ voxels with voxel size $1 \text{ mm} \times 1 \text{ mm} \times 1 \text{ mm}$. Using a model of this size allows us to maintain a balance between accuracy and required computation resources.

The last step of the algorithm is to convert models in STL format files for further imports into FEM simulation software. In order to convert voxel models to STL format, each model is divided into a set of binary voxel 3D-matrices. Each binary voxel 3D-matrix for a certain type of biological tissue contains a non-zero elements in the respective elements of these biological tissue of the voxel 3D-matrix.

Each binary voxel 3D-matrix is divided into connected components with connectivity set to 6. Each connected component is stored in the form of geometric bodies in separate STL file. The number of geometrical bodies after saving was 172. The number of unique types of biological tissue after save was 21.

After saving as a set of STL-files, the model of human neck was imported into the COMSOL Multiphysics 5.2a software. After the meshing procedure, imported geometry model was presented in the form of 1.5 million tetrahedra.

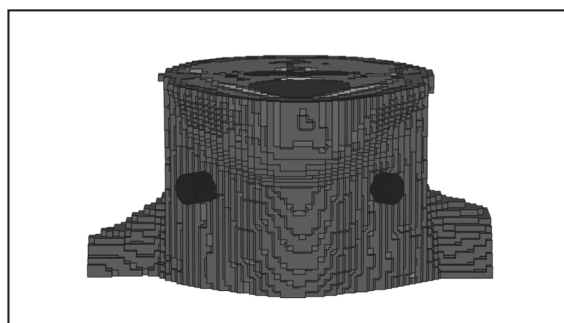


Figure 5: Appearance of the human neck 3D-model.

Each imported geometric body was set to its appropriate biological tissue. All in all, the following types of biological tissues were used: Blood, Bone, Cerebrospinal Fluid, Connective Tissue, Esophagus, Fat, Intervertebral disc, Larynx, Mandible, Bone marrow red, Mucous, Muscle, Nerve, Subcutaneous adipose tissue (SAT), Spinal Cord, Skin, Tendon Ligament, Thyroid Gland, Tongue, Trachea, Vertebrae. For each biological tissue in the model physical characteristics were set based on IT'IS Database for thermal and electromagnetic parameters of biological tissues (Hasgall *et al.*, 2012). The following physical characteristics were set: electrical conductivity, relative permittivity, density, heat capacity, thermal conductivity, blood perfusion rate, heat generation rate. Values of relative permittivity and electrical conductivity physical characteristics were set to be frequency dependent in range from 1 Hz to 100 MHz. Therefore, the developed model took into account the peculiarities of the formation of thermal effects with the use of pulsed current.

2.3 Model Configuration

The electrode system in model is represented by two cylindrical brass electrodes with 15 mm in diameter and 10 mm thickness. The conductivity of brass is much greater than the conductivity of the biological tissues. Therefore, accurate transmission of the real electrode geometry to model is not needed. The single requirement to the model electrode is equality of model electrode diameter to real electrode diameter (Kublanov and Babich, 2015).

Appearance of the human neck 3D-model with placed electrodes is shown in Fig. 5. The electrode placement on Fig. 5 corresponds to one of the possible variants of the partial current formation. The left electrode is used as anode, and the right electrode is used as cathode. The electrodes are marked in the image in black.

For the model calculation, frequency stationary study was used. This study calculates temperature distribution by the model volume at thermal equilibrium.

Temperature on boundaries, which were formed after truncating model to the human's neck area, was set to 310 K.

For simulation, the frequency range from 1 Hz to 100 MHz was used. This range includes first 20000 harmonics of the neuro-electrostimulation signal. Low-frequency components contain significantly greater amount of energy than high. Therefore, the frequency range for simulation was set to a logarithmic scale as follows: (1, 3, 5, 7, 9, 10, 30, 50, 70, 90, 100, 300, 500, 700, 900, 1k, 3k, 5k, 7k 9k, 10k, 30k, 50k, 70k, 90k, 100k 300k, 500k, 700k, 900k, 1M, 3M, 5M, 7M, 9M, 10M, 30M, 50M, 70M, 90M 100M) Hz.

For simulation, amplitude of the harmonic current components was set to 10 mA. Although it is possible to conduct simulation with other values of the current.

In addition, we studied model without applied partial currents. These results were used for the base of the temperature distribution in human tissues in the neck in the absence of neuro-electrostimulation signal.

After computation of the models for all harmonics, temperatures values depending on the coordinates x, y, z were exported into *.csv files. Each frequency corresponds to a separate *.csv file.

2.4 Preparation of Thermal Difference Results

Python script has been written for the calculation and analysis of the thermal changes during the neuro-electrostimulation process on the basis of equation 6, using the previously exported temperature distributions, saved in set of *.csv files. This script performs the following steps:

- import of the *.csv files and convert them to the form of thermal distribution 3D-matrices;
- calculation of amplitudes and frequencies of the Fourier series harmonics of the periodic pulsed signal used for neuro-electrostimulation;
- 3D-matrix calculation of thermal changes for each harmonic used in simulation;
- interpolation of existing thermal changes 3D-matrices for decomposed harmonic frequencies used for neuro-electrostimulation signal;
- summation of 3D-matrix thermal changes for each decomposed harmonic of neuro-

electrostimulation in accordance with equation 6.

The results of script execution are thermal changes for the whole model volume depending on neuro-electrostimulation pulse characteristics was calculated.

3 RESULTS

The cross-section of the thermal increase distribution of tissues human neck during neuro-electrostimulation processes is shown in Fig. 6. Neuro-electrostimulation pulse characteristics were: 1 mA amplitude, 30 us duration, and 50 Hz frequency. The vertical level of the image is selected the same as in Fig. 1.

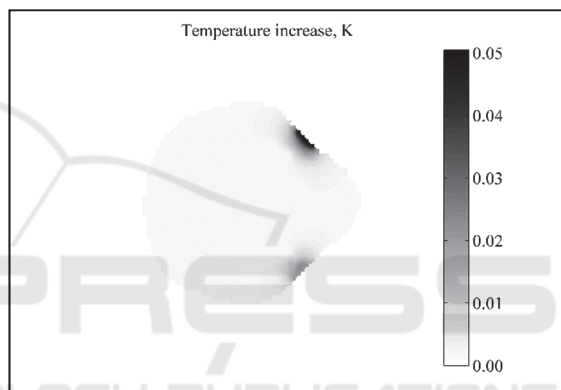


Figure 6: The cross-section of temperature increase in the human neck for neuro-electrostimulation current pulse characteristics 1 mA amplitude, 30 us duration, and 50 Hz frequency.

According to the image in the Fig. 6, the maximum temperature increase (0.05 K) is located at cathode and anode application points. Significant thermal increase were not observed in the inner biological tissues of neck area This can explained by a decrease of the current density with increasing depth of biological tissue location. One can note that the maximal thermal increase under the cathode and the anode are different. That can be explained by the different thicknesses of the skin in electrode application points of the Duke model. For human neck model with a constant thickness of the skin difference of maximum thermal increase under the cathode and anode application points will not be observed.

Maximal thermal increase was considered as the integral parameter of thermal effects in the entire

volume of biological tissues caused by neuro-electrostimulation.

Maximal thermal increase in biological tissues of the human neck using neuro-electrostimulation dependency on the signal duration and frequency for the 1 mA pulse amplitude is shown in Fig. 7. Maximum thermal increase in biological tissues of the human neck using neuro-electrostimulation dependency on the signal duration and frequency for the 15 mA pulse amplitude is shown in Fig. 8.

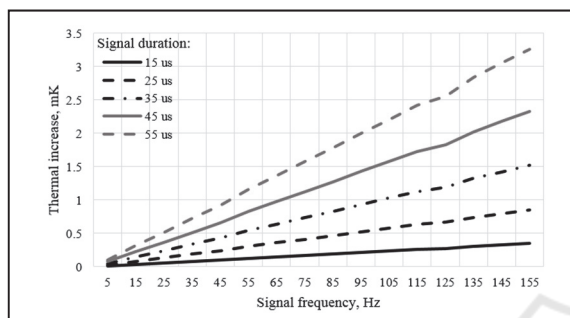


Figure 7: Maximal thermal increase against frequency, for different durations, for the 1 mA pulse amplitude.

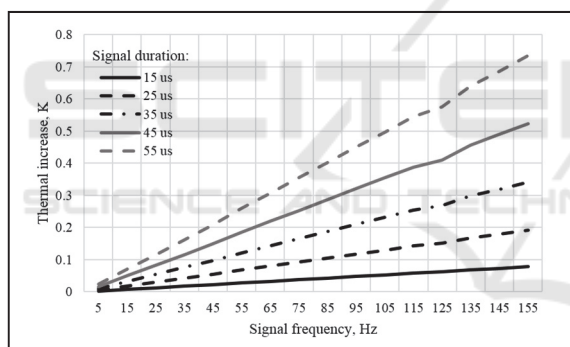


Figure 8: Maximal thermal increase against frequency, for different durations, for the 15 mA pulse amplitude.

Fig. 7 and Fig. 8 show that maximal thermal increase for 1 mA pulse amplitude is 3.5 mK and for 15 mA is 0.7 K. Comparison of the plots, presented on Fig. 7 and Fig. 8 reveal quadratic dependency of the maximal temperature on pulse current amplitude. The thermal increase caused by the neuro-electrostimulation, becomes stronger, as the pulse modulation frequency and pulse duration increase. This can be explained by the fact that the heating of the tissues magnifies with the increase of the neuro-electrostimulation duty-cycle.

Let us consider the maximal permissible current for different stimulation pulse duration and frequency characteristics with the condition: the maximal thermal increase in the volume of biological tissue

does not exceed the 0.1 K. The tissue heating less than 0.1 K is considered non-thermal exposure and cannot cause tissue damage (WHO | Electromagnetic fields and public health 2016). Plot of the neuro-electrostimulation current pulse amplitude against frequency, for different pulse duration, under condition that the maximum thermal rise in human tissues of the neck is less than 0.1 K is shown in Fig. 9.

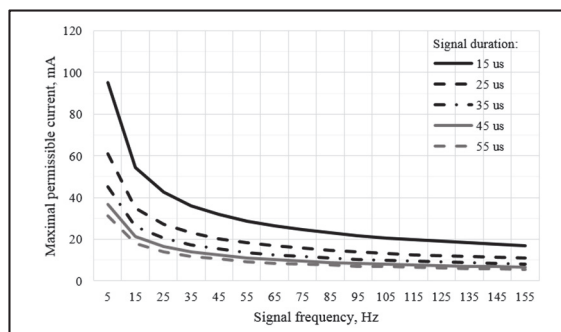


Figure 9: Maximal permissible current against frequency, for different durations.

According to the Fig. 9 the application of the pulse current with the frequencies in range 45-55 Hz, duration 25-30 us and amplitude less than 13 mA, will not cause significant thermal effects. These pulse current features are the most frequently used ones for the neuro-electrostimulation processes. For application of the pulse current with higher frequencies, one must reduce duration and amplitude in order to prevent significant tissue heating.

4 CONCLUSIONS

The current work presented methodology of the FEM simulation for thermal effects evaluation, caused by the neck region neuro-electrostimulation. Algorithm of the voxel model conversion to the 3-D objects represented as the complex of the STL-files was described. The evaluation of the temperature in the biological tissues is based on the association of the partial thermal changes, caused by the harmonics components of the pulsed neuro-electrostimulation signal.

Features of the thermal changes in the neck region were considered for the neuro-electrostimulation by means of the current pulse field formed in the "SYMPATHOCOR-01" device. Results have shown that for modulation frequencies in range 45-55 Hz, duration of the partial pulses 25-30 us, current pulse amplitude less than 13 mA, the neuro-

electrostimulation does not cause thermal changes higher than 0.1 K.

In our future works, it is planned to carry out verification of the heat distribution model in the laboratory. Also in plans, to assess the impact of deviations of the biological tissue physical characteristics on the temperature distribution.

The developed methodology of the thermal effects assessment caused by pulsed current neuro-electrostimulation in the human neck will allow to develop guidelines for choosing the parameters of the current pulses field for each patient, taking into account his anthropometric characteristics.

The height and body mass index (BMI) will be used as the anthropometric characteristics of the patient. It is assumed based on these characteristics, a doctor will select appropriate model from a set of a Virtual Population model group and then will produce linear transformation of the model to meet the patient's height and BMI. Then, based on the calculated model it is suggested to recommend ranges of stimulation parameters.

ACKNOWLEDGMENTS

The work was supported by Act 211 Government of the Russian Federation, contract № 02.A03.21.0006.

REFERENCES

- Arfken, G.B., Weber, H.J., and Harris, F.E., 2011. *Mathematical methods for physicists: a comprehensive guide*. Academic press.
- Bergman, T.L. and Incropera, F.P., 2011. *Introduction to heat transfer*. John Wiley & Sons.
- Bergman, T.L., Incropera, F.P., DeWitt, D.P., and Lavine, A.S., 2011. *Fundamentals of heat and mass transfer*. John Wiley & Sons.
- Cao, X., Sui, X., Lyu, Q., Li, L., and Chai, X., 2015. Effects of different three-dimensional electrodes on epiretinal electrical stimulation by modelling analysis. *Journal of neuroengineering and rehabilitation*, 12 (1), 1.
- Christ, A., Kainz, W., Hahn, E.G., Honegger, K., Zefferer, M., Esra Neufeld, Rascher, W., Janka, R., Bautz, W., Chen, J., Kiefer, B., Schmitt, P., Hans-Peter Hollenbach, Shen, J., Oberle, M., Szczerba, D., Kam, A., Guag, J.W., and Kuster, N., 2010. The Virtual Family—development of surface-based anatomical models of two adults and two children for dosimetric simulations. *Physics in Medicine and Biology*, 55 (2), N23.
- Gonzalez-Diaz, R., Jimenez, M.-J., and Medrano, B., 2015. 3D well-composed polyhedral complexes. *Discrete Applied Mathematics*, 183, 59–77.
- Hasgall, P.A., Neufeld, E., Gosselin, M.C., Klingenböck, A., and Kuster, N., 2012. IT'IS Database for thermal and electromagnetic parameters of biological tissues. *IT'IS Foundation website*.
- Kublanov, V.S., 2008a. A hardware-software system for diagnosis and correction of autonomic dysfunctions. *Biomedical Engineering*, 42 (4), 206–212.
- Kublanov, V.S., 2008b. [A hardware-software system for diagnosis and corrections of autonomic dysfunctions]. *Meditsinskaia tekhnika*, (4), 40–46.
- Kublanov, V.S. and Babich, M.V., 2015. Principles of organization and control of multielectrode neuro-electrostimulation device. In: *Biomedical Engineering and Computational Technologies (SIBIRCON), 2015 International Conference on*. IEEE, 82–86.
- Laughton, M.A. and Warne, D.F., 2002. *Electrical Engineer's Reference Book*. Newnes.
- Netter, F.H., 2010. *Atlas of human anatomy*. Elsevier Health Sciences.
- Su, Y., Souffrant, R., Kluess, D., Ellenrieder, M., Mittelmeier, W., van Rienen, U., and Bader, R., 2014. Evaluation of electric field distribution in electromagnetic stimulation of human femoral head. *Bioelectromagnetics*, 35 (8), 547–558.
- WHO | Electromagnetic fields and public health: radars and human health [online], 2016. WHO. Available from: <http://www.who.int/peh-emf/publications/facts/fs226/en/> [Accessed 21 Oct 2016].